

Experimental investigation of distributions of the off-diagonal elements of the scattering matrix and Wigner's \hat{K} matrix for networks with broken time reversal invariance

Michał Ławniczak ¹, Bart van Tiggelen ² and Leszek Sirko ¹

¹*Institute of Physics, Polish Academy of Sciences, Aleja Lotników 32/46, 02-668 Warsaw, Poland*

²*University Grenoble Alpes, CNRS, LPMMC, 38000 Grenoble, France*



(Received 8 July 2020; accepted 3 November 2020; published 23 November 2020)

We present an extensive experimental study of the distributions of the real and imaginary parts of the off-diagonal elements of the scattering matrix \hat{S} and the Wigner's reaction \hat{K} matrix for open microwave networks with broken time (T) reversal invariance. Microwave Faraday circulators were applied in order to break T invariance. The experimental distributions of the real and imaginary parts of the off-diagonal entries of the scattering matrix \hat{S} are compared with the theoretical predictions from the supersymmetry random matrix theory [A. Nock, S. Kumar, H.-J. Sommers, and T. Guhr, *Ann. Phys. (NY)* **342**, 103 (2014)]. Furthermore, we show that the experimental results are in very good agreement with the recent predictions for the distributions of the real and imaginary parts of the off-diagonal elements of the Wigner's reaction \hat{K} matrix obtained within the framework of the Gaussian unitary ensemble of random matrix theory [S. B. Fedeli and Y. V. Fyodorov, *J. Phys. A: Math. Theor.* **53**, 165701 (2020)]. Both theories include losses as tunable parameters and are therefore well adapted to the experimental verification.

DOI: [10.1103/PhysRevE.102.052214](https://doi.org/10.1103/PhysRevE.102.052214)

I. INTRODUCTION

Quantum chaotic scattering was introduced almost 70 years ago to describe properties of large scale complicated quantum systems [1–3]. The significant role of broken time-reversal in quantum chaos [4] is undoubtedly one of the most remarkable discoveries. It is generally acknowledged that controllable experimental investigations of complex quantum systems are difficult to perform due to decoherence, therefore, the multitude of physical problems from the field of quantum chaos can be tackled experimentally with the help of microwave networks simulating quantum graphs [5–7].

This article demonstrates how microwave networks can be applied to obtain the first experimental results on the distributions of off-diagonal elements of the scattering matrix \hat{S} and the Wigner's reaction \hat{K} matrix for systems with broken time-reversal invariance. The experimental results are compared to the recent exact random matrix theory (RMT) solutions of these problems [8,9].

Quantum graphs consisting of one-dimensional wires connected by vertices were introduced by Pauling [10]. They can be considered as idealizations of physical networks in the limit where the widths of the wires are much smaller than their lengths [11]. Quantum graphs constitute rich tools for the study of open quantum systems which exhibit chaotic scattering [12–14]. They have been used to describe a large variety of systems and models, e.g., quantum circuits in tunnel junctions [15], superconducting quantum circuits [16], realization of high-dimensional multipartite quantum states [17] and discrete-time models of quantum gravity [18].

Quantum graphs can be simulated by microwave networks because there is a direct analogy between the Schrödinger equation applied to a quantum graph and the telegraph equation of the corresponding microwave network [5]. Mi-

crowave networks can be specially designed to allow for the experimental realization of systems corresponding to all three fundamental ensembles in the random matrix theory: the Gaussian orthogonal ensemble (GOE, symmetry index $\beta = 1$ in RMT) [5,13,19–22] and the Gaussian symplectic ensemble (GSE, symmetry index $\beta = 4$) [23–25] which are both characterized by T invariance, as well as the Gaussian unitary ensemble (GUE, symmetry index $\beta = 2$) [6,7,23–27] for which T invariance is broken.

The prediction of supersymmetry for the distribution of off-diagonal entries of the scattering matrix \hat{S} for systems with losses was given in Refs. [8,28] and compared with data from T -invariant microwave cavities [28]. The theoretical prediction for the full statistics of the off-diagonal cross sections for T -invariant and T -violated systems were calculated exactly by Kumar *et al.* [29] but the confrontation to data could only be done for a microwave cavity and a compound nucleus that has T invariance obeyed. The first study of off-diagonal elements of the scattering matrix in open cavities with broken T invariance was done by Dietz *et al.* [30], where the distributions of the modulus of the measured off-diagonal \hat{S} -matrix element S_{ba} for a flat superconducting microwave billiard with weakly broken time-reversal T invariance were compared to RMT simulations.

II. WIGNER'S REACTION \hat{K} MATRIX

Although chaotic open systems with T invariance (GOE systems) have been investigated in most of their aspects, the theoretical investigations of the Wigner's reaction \hat{K} matrix were initially concentrated on the distributions $P(v)$ and $P(u)$ of the imaginary and the real parts of its diagonal elements [31,32]. The Wigner's reaction \hat{K} matrix is a very

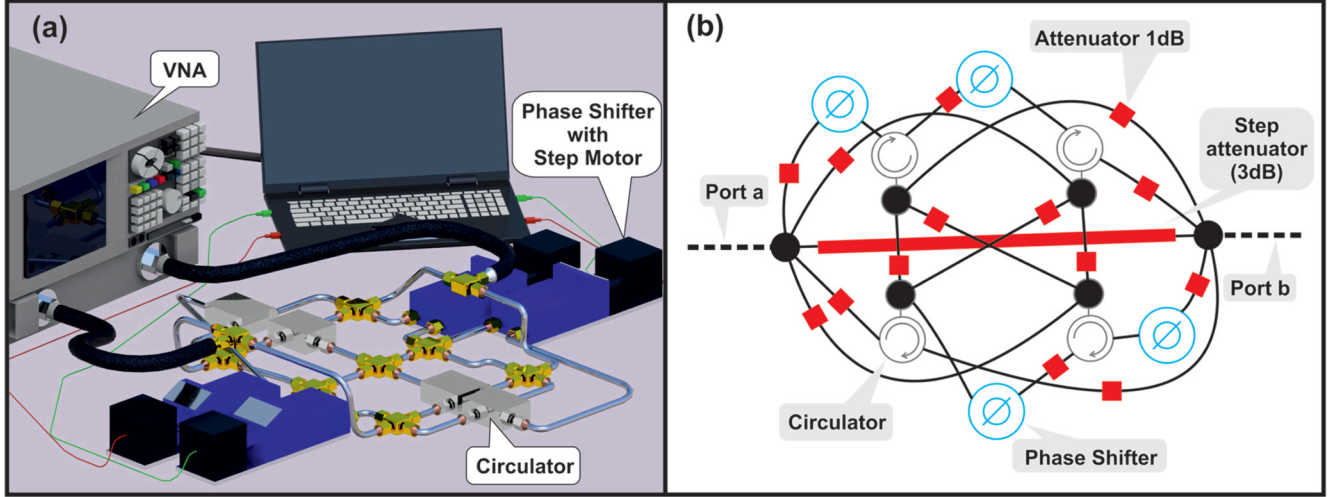


FIG. 1. (a) The experimental setup for measuring the scattering matrix \hat{S} of the microwave networks with violated T invariance and intermediate value of the parameter γ . The network consists of nine microwave joints. Different realizations of the network were obtained using four phase shifters. The T violation was induced with four Anritsu PE8403 microwave circulators. (b) The experimental setup for measuring the scattering matrix \hat{S} of the hexagon microwave networks with violated T invariance and large parameter γ . Also here, different realizations of the network were obtained using four phase shifters and T violation was induced with four Anritsu PE8403 microwave circulators. The matrix \hat{S} was measured at the inputs of the six-joint vertices.

important observable operator of an open system because it links the properties of *closed* chaotic systems, described by a Hamiltonian exhibiting quantum chaos, to the properties of the corresponding *open* system where irreversible scattering occurs towards the environment outside. The theoretical findings [31,32] were confirmed with very good precision in the experiments using microwave networks [13,33] and microwave cavities [34,35].

Recently the first experimental results were also reported for the GUE systems [7]. In this case the distributions of the diagonal elements of the 2×2 Wigner's reaction matrix \hat{K} were investigated for the large parameter $\gamma = 2\pi\Gamma/\Delta \geq 19.4$, where Γ and Δ are the average width of resonances caused by both absorption and leaks and the mean level spacing, respectively. Since Γ depends on absorption, it is a parameter that is relatively easy to control experimentally with microwave networks.

In the recent paper [9] the off-diagonal entries K_{ab} of the Wigner's reaction \hat{K} matrix were theoretically studied for chaotic systems with T invariance either broken or not, and for arbitrary losses. The paper [9] generalizes the results of Ref. [36] where T -invariant and T -violated systems in the limiting case of zero absorption were studied. The distribution of the modulus squared of the off-diagonal elements $|K_{ab}|^2$ for chaotic graphs with broken T invariance was derived in Ref. [37].

Diagonal entries to the Wigner reaction matrix \hat{K} have recently been observed for microwave networks with violated time-reversal invariance in the case of large losses [7]. Contrary to the diagonal entries of \hat{K} , the off-diagonal elements of \hat{K} have not been investigated experimentally yet.

The distributions of the off-diagonal elements K_{ab} and K_{ba} of the 2×2 reaction \hat{K} matrix can be obtained from the two-port scattering matrix \hat{S} of the network after elimination of

direct processes, which are not chaotic [38–40]

$$\hat{K} = i \frac{\hat{S} - \hat{I}}{\hat{S} + \hat{I}}. \quad (1)$$

The matrix \hat{I} denotes the 2×2 identity matrix. The matrix \hat{K} is related to the normalized impedance \hat{z} [38]: $\hat{K} = -i\hat{z}$ and is Hermitian only without absorption.

III. MICROWAVE NETWORKS WITH BROKEN TIME-REVERSAL INVARIANCE

In this article we consider microwave networks with broken time-reversal invariance and characterized by intermediate and large width of the resonances $\gamma > 5.39$. For such large values conventional indicators for T violation such as short- and long-range spectral correlation functions [41], the nearest neighbor level spacing distribution or the spectral rigidity are very difficult, if not impossible to use because individual levels are hardly distinguishable. Therefore, we will bypass this severe problem using the enhancement factor W [6] as a probe of broken time-reversal.

Microwave networks consist of vertices (microwave joints) connected by edges, realized by coaxial SMA-RG402 cables. The SMA-RG402 coaxial cable contains a center conductor of radius $r_1 = 0.05$ cm surrounded by a Teflon insulating layer having a dielectric constant $\epsilon \simeq 2.06$ [42]. The insulating layer is surrounded by a tubular conductor of radius $r_2 = 0.15$ cm. Inside a coaxial cable and below the cut-off frequency of the TE_{11} mode only the fundamental transverse-electromagnetic (TEM) mode can propagate. The TE_{11} mode cut-off frequency for the SMA-RG402 coaxial cable is $\nu_{\text{cut}} \simeq \frac{c}{\pi(r_1+r_2)\sqrt{\epsilon}} \simeq 33$ GHz [43], where c is the speed of light in the vacuum. Absorption of the networks was controlled by

changing the total lengths of the networks and adding to the networks microwave 1 dB and 3 dB attenuators.

The two-port scattering matrix \hat{S} of the nine-vertex and six-vertex microwave networks required for the evaluation of the Wigner's matrix \hat{K} and the enhancement factor W was measured using the setups shown in Figs. 1(a) and 1(b), respectively. The T violation was induced by four Anritsu PE8403 microwave Faraday circulators with low insertion loss which operate in the frequency range 3–7 GHz. The microwave circulators are nonreciprocal three-port passive devices. A wave entering the circulator through port 1, 2, or 3 exits at port 2, 3, or 1, respectively, as shown schematically in Fig. 1(a).

For Neumann-Kirchhoff boundary conditions [44] in order to keep a quantum-microwave vertex analogy the microwave vertex scattering matrices $\hat{S}_v(\nu)$ and $\hat{S}_v(\nu_0)$ at frequencies ν and ν_0 should be related by the equation [45–48]

$$\hat{S}_v(\nu) = \frac{(\nu + \nu_0)\hat{S}_v(\nu_0) + (\nu - \nu_0)\hat{I}}{(\nu + \nu_0)\hat{I} + (\nu - \nu_0)\hat{S}_v(\nu_0)}. \quad (2)$$

Here, the matrix \hat{I} denotes the identity matrix of the dimension of the vertex scattering matrices $\hat{S}_v(\nu)$ and $\hat{S}_v(\nu_0)$. It can be easily checked for example that for the microwave T junctions used in the construction of the nine-vertex microwave network, which possess three equivalent ports, the matrix $\hat{S}_v(\nu_0)$ is unitary and Hermitian

$$\hat{S}_v(\nu_0) = \frac{1}{3} \begin{pmatrix} -1 & 2 & 2 \\ 2 & -1 & 2 \\ 2 & 2 & -1 \end{pmatrix}, \quad (3)$$

so that $\hat{S}_v^2(\nu_0) = \hat{I}$. Then Eq. (2) is equivalent to $\hat{S}_v(\nu) = \hat{S}_v(\nu_0)$. Indeed, our T junctions to a very good approximation are independent on frequency ν .

A microwave circulator in the operating frequency range $\nu \in [3, 7]$ GHz defines a vertex which can be described by the scattering matrix

$$\hat{S}_v = \begin{pmatrix} 0 & 0 & 1 \\ 1 & 0 & 0 \\ 0 & 1 & 0 \end{pmatrix}. \quad (4)$$

This matrix is unitary but not Hermitian as is required by the vertex boundary conditions of a quantum graph specified by Eq. (2), and therefore Eq. (2) imposes a frequency dependence that does not exist in a microwave circulator. As a result, a microwave circulator can be considered analogous to a quantum vertex when the frequency bandwidth enforces $\hat{S}_v(\nu) \simeq \hat{S}_v(\nu_0) = \hat{S}_v$. In practice, to preserve quantum analog properties of the networks with violated T symmetry, the operating frequency range 3–7 GHz was divided into 13 intervals of width $\Delta\nu = 307.69$ MHz, where $\hat{S}_v(\nu) \simeq \hat{S}_v(\nu_0)$.

The ensembles of different microwave networks realizations were created by changing the lengths of four edges of the networks using the phase shifters visible in Figs. 1(a) and 1(b) in such a way that the total “optical” lengths of the networks were preserved. The hexagon network shown in Fig. 1(b) was built to investigate networks with larger parameter γ and with larger total “optical” length than the nine-vertex network. To increase even further the internal absorption of the network in order to verify the theory [9] in the limit of large losses, 1 dB

attenuators were used on its 14 edges. The direct processes on the edge connecting directly the two six-joint vertices (ports a and b of the network) were minimized by applying a 3 dB step attenuator. The total “optical” length of the nine-vertex network including edges, phase shifters, joints, and circulators, was 361 cm while the total “optical” length of the hexagon, 6-vertex network, including all previous components and 1 dB and 3 dB attenuators was 662 cm. The scattering matrix \hat{S} of the networks was measured in the frequency range 3–7 GHz by a vector network analyzer (VNA), Agilent E8364B. The microwave networks were connected to the VNA through the leads—flexible microwave cables HP 85133-616 and HP 85133-617. The experimental results were obtained by averaging over 1500 and 983 realizations of the nine-vertex network without attenuators and the hexagon network containing 1 dB and 3 dB attenuators, respectively.

The analogy between microwave networks with broken T -invariance and quantum graphs is merely done on random matrix level [6,24,26,27]. Here, however, in the analysis of the experimental results, to keep the properties of the networks with violated T symmetry as close as possible to their quantum analogs, taking into account properties of microwave circulators, the operating frequency range 3–7 GHz was divided further up into 13 intervals of width $\Delta\nu = 307.69$ MHz, where $\hat{S}_v(\nu) \simeq \hat{S}_v(\nu_0)$. The distributions of the real and imaginary parts of the off-diagonal elements of the scattering matrix \hat{S} and the Wigner's reaction \hat{K} matrix were separately calculated in each individual interval and averaged over all intervals.

The elastic enhancement factor W [6,40,49–51] was used to monitor T symmetry of the investigated systems. It can be obtained from the two-port scattering matrix \hat{S} using the following relation:

$$W = \frac{\sqrt{\text{var}(S_{aa})\text{var}(S_{bb})}}{\text{var}(S_{ab})}, \quad (5)$$

where $\text{var}(S_{ab}) \equiv \langle |S_{ab}|^2 \rangle - |\langle S_{ab} \rangle|^2$ denotes the variance of the matrix element S_{ab} . For intermediate and large parameter γ the enhancement factor W is predicted to depend weakly on its value but is very sensitive to the ensemble [40], approaching for $\gamma \rightarrow +\infty$ the limit of $W = 2/\beta$.

IV. EXPERIMENTAL DISTRIBUTIONS OF THE REAL AND IMAGINARY PARTS OF THE SCATTERING MATRIX S_{ab}

The exact results for the distributions of the real $P(x_1)$ and imaginary $P(x_2)$ parts of S_{ab} in the framework of the supersymmetry RMT were obtained by Nock *at al.* [8]. In the $\beta = 2$ case the distributions are identical and are given by the formulas (55-56) in Ref. [8]. These formulas depend on the antenna transmission coefficients T_a and T_b , where $T_m = 1 - |\langle S_{mm} \rangle|^2$ for $m = a, b$ [40,49], and the transmission coefficients of M parasitic absorption and leak channels T_c . Using the Weisskopf estimate [49] the parameter γ characterizing the distributions $P(x_i)$ can be found in our case from the formula $\gamma = T_a + T_b + \sum_{c=1}^M T_c$, where $M \gg 1$.

In Fig. 2(a) the experimental distributions of the real $P(x_1)$ and imaginary $P(x_2)$ parts of the off-diagonal element of the scattering matrix S_{ab} , black full circles and black triangles, re-

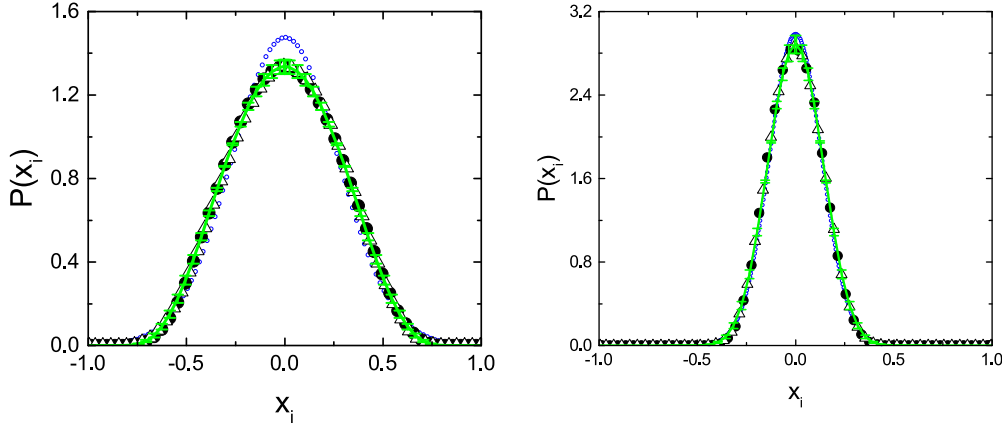


FIG. 2. (a) Experimentally evaluated distributions $P(x_1)$ and $P(x_2)$ of the real (black full circles) and imaginary (black triangles) parts of S_{ab} in the $\beta = 2$ case at $\gamma = 5.39 \pm 0.23$. The theoretical fit with marked standard errors is denoted by green broken line. The Gaussian approximation is marked with small blue circles. (b) depicts the same quantities for $\gamma = 25.77 \pm 1.43$.

spectively, are shown for the microwave networks with broken T invariance. The fit of theory to data with $\gamma = 5.39 \pm 0.23$, corresponding to weakly overlapping resonances, is shown as a green broken line. This value of γ was fitted for $M = 100$ independent identical effective open channels with the transmission coefficient T_c using the formulas (46-47) and (55-56) in Ref. [8]. As the input parameters the antenna transmission coefficients $T_a = T_b = 0.89 \pm 0.05$ were used. The fit yielded the value $T_c = 0.0361 \pm 0.013$. Then using the Weisskopf estimate we obtained $\gamma = T_a + T_b + \sum_{c=1}^M T_c = T_a + T_b + MT_c = 5.39 \pm 0.23$. As demonstrated in Ref. [52] the exact number of channels M is not of relevance provided that $M \gg 1$. Indeed, we checked that already for $M \geq 50$ one obtains the same value of $\gamma = 5.39 \pm 0.23$. The antenna transmission coefficients $T_a = T_b = 0.89 \pm 0.05$ were evaluated using the formula $T_m = 1 - |\langle S_{mm} \rangle|^2$ utilizing experimentally measured scattering matrix elements S_{mm} , where $m = a, b$.

We used Matlab *compare* and NRMSE functions to find the goodness of fit (GF) between the observed distributions and the theoretical model [8]. For the distributions of the real $P(x_1)$ and imaginary $P(x_2)$ parts the off-diagonal element of the scattering matrix S_{ab} , GF was 98.6% and 97.8%, respectively. For a value $\gamma = 5.39 \pm 0.23$ the observed statistics deviate strongly and with low uncertainty from the Gaussian approximation (small blue circles).

In Fig. 2(b) we show the measured distributions $P(x_i)$ of the real (black full circles) and imaginary (black triangles) parts of S_{ab} compared to the theoretical (green broken line) obtained for $\gamma = 25.77 \pm 1.43$, which approaches the Ericson regime of strongly overlapping resonances. The parameter γ was fitted for $M = 100$ channels and $T_a = T_b = 0.58 \pm 0.05$, yielding $T_c = 0.246 \pm 0.013$. Here, GF was calculated to be 98.6% and 98.3%, respectively. In this case the Gaussian approximation (small blue circles) is much closer to the theoretical and experimental results. For both weakly and strongly overlapping resonances, the experimental results are in excellent agreement with the theoretical predictions confirming accurately the validity of the theory exploiting the Heidelberg approach [8].

In Table I the enhancement factor W of the scattering matrix \hat{S} of the microwave networks measured for two experimental values of the parameter γ is compared to the theoretical prediction W_{th} . The enhancement factor W_{th} was calculated using Eq. (5) by applying the formulas (19) in Ref. [49] for the variances of the scattering matrix elements S_{ij} . In the calculations we used the transmission coefficients $T_a = 0.89 \pm 0.05$ and $T_b = 0.89 \pm 0.05$, and $T_a = 0.58 \pm 0.05$ and $T_b = 0.58 \pm 0.05$ for the networks with intermediate and large parameter γ , respectively. Next, the internal absorption parameter γ_{int} of the networks was calculated from $\gamma_{int} = \gamma - T_a - T_b$, which is equivalent to the sum over the transmission coefficients T_c , $\gamma_{int} = \sum_{c=1}^M T_c$. The agreement of the experimental and theoretical results clearly shows that both networks have fully developed chaos with broken T invariance. Such properties of the microwave networks are not surprising because for the networks with broken T invariance and with relatively small absorption, so that the individual eigenvalues are easily identified, the level spacing distribution is in good agreement with the GUE prediction in RMT [6,24,26,27]. Moreover, this agreement also extends to the case of missing levels. The fluctuation properties in incomplete spectra of microwave networks are in excellent agreement with the theoretical GUE predictions in RMT for missing levels statistics [27]. In addition, a set of two chaotic microwave networks with broken time reversal symmetry can be used to construct chaotic microwave networks with GSE properties [23,24]. In the case of larger absorption other indicators of chaoticity such as the diagonal elements of the

TABLE I. The experimental enhancement factor W of the microwave networks equipped with Faraday circulators compared to the theoretical predictions W_{th}^{GUE} and W_{th}^{GOE} for GUE and GOE systems, respectively, for two experimental values of the parameter γ .

γ	W	W_{th}^{GUE}	W_{th}^{GOE}
5.39 ± 0.23	1.23 ± 0.22	1.28	2.19
25.77 ± 1.43	1.13 ± 0.12	1.07	2.04

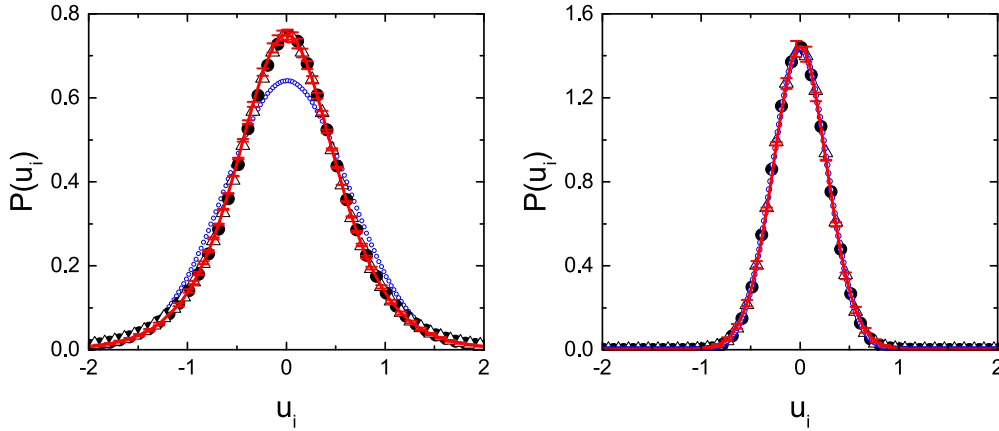


FIG. 3. (a) Experimentally evaluated distributions $P(u_1)$ and $P(u_2)$ of the real (black full circles) and imaginary (black triangles) parts of K_{ab} in the $\beta = 2$ case at $\alpha = \gamma/4 = 1.35 \pm 0.06$. The theoretical results are denoted by red broken line. The error bars mark the errors caused by the $\gamma = 5.39 \pm 0.23$ uncertainty. The Gaussian approximation is marked with small blue circles. Panel (b) depicts the same quantities for $\alpha = \gamma/4 = 6.44 \pm 0.36$. The error bars mark the errors caused by the $\gamma = 25.77 \pm 1.43$ uncertainty while the Gaussian approximation is marked with small blue circles.

Wigner's reaction matrix [22] or the enhancement factor [6] were used to demonstrate that microwave networks with microwave circulators behave as ensembles with violated T symmetry.

V. EXPERIMENTAL DISTRIBUTIONS OF THE OFF-DIAGONAL ELEMENTS OF THE WIGNER'S REACTION \hat{K} MATRIX

We now turn to the observation of the statistics of the off-diagonal elements of the Wigner's \hat{K} matrix. According to the work of Fedeli and Fyodorov [9], the joint probability density function associated with complex Hermitian GUE matrices \hat{H}_N of size $N \times N$, in the limit $N \rightarrow \infty$, is given by

$$P(\text{Re}K_{ab}, \text{Im}K_{ab}) = \frac{\alpha^2}{\pi} \lim_{x \rightarrow 2\pi\rho(\lambda)\alpha} D_x \frac{\exp(-\sqrt{x^2 + 4\alpha^2|K_{ab}|^2})}{\sqrt{x^2 + 4\alpha^2|K_{ab}|^2}}, \quad (6)$$

where $\text{Re}K_{ab}$ and $\text{Im}K_{ab}$ are the real and imaginary parts of the off-diagonal element K_{ab} and the operator $D_x = \sinh(x)(1 + \frac{d^2}{dx^2}) - 2 \cosh(x) \frac{d}{dx}$. Equation (6) is parameterized by the parameter α and the spectral density given by the Wigner's semicircular law $\rho(\lambda) = \frac{1}{2\pi} \sqrt{4 - \lambda^2}$.

In the model considered in [9] the losses are taken into account by allowing the spectral parameter (energy) λ to achieve an imaginary part by replacing $\lambda \rightarrow \lambda + i\alpha/N$ equal for all N modes. The correspondence between the parameter α and the parameter γ can be established using the fact that the losses in a physical system such as absorption and the effect of openness can equivalently be taken into account by a purely imaginary shift of the scattering energy $\epsilon \rightarrow \epsilon + \frac{i}{2}\Gamma$, where Γ is the average width of resonances ϵ [40].

An estimate for the value for α of our network can be determined by comparison of the rescaled widths of the spectral parameter $\frac{\alpha}{N\Delta_m}$ and resonances $\frac{\Gamma}{2\Delta}$, which leads to a simple

relationship between γ and α ,

$$\gamma = 2\pi\Gamma/\Delta = 4\pi\rho(\lambda)\alpha, \quad (7)$$

where $\Delta_m = 1/(N\rho(\lambda))$ [8] is the mean level spacing of GUE eigenvalues.

The probability density function for the variables $u_1 = \text{Re}K_{ab}$ and $u_2 = \text{Im}K_{ab}$ can be numerically evaluated upon performing the integral

$$P(u_i) = \int_{-\infty}^{+\infty} P(u_1, u_2) du_i. \quad (8)$$

The distributions $P(u_i)$ as well as Eq. (6) depend on the parameters $\rho(\lambda)$ and α . However, in the limit $N \rightarrow \infty$ it is sufficient to stay in the center of the semicircle [53] where the spectral density of GUE eigenvalues is given by $\rho(0) = 1/\pi$. Hence, using Eq. (7) we can express the parameter α in Eq. (6) as $\alpha = \gamma/4$. In this way the theoretical distributions given by Eq. (8) can be compared directly to the experimental distributions $P(u_i)$ of the real and imaginary parts of the off-diagonal entries of the Wigner's \hat{K} matrix.

In Fig. 3(a) the experimental distributions $P(u_1)$ and $P(u_2)$ of the real and imaginary parts of the off-diagonal element K_{ab} of the Wigner's reaction \hat{K} matrix, denoted by black full circles and black triangles, respectively, are shown for the microwave networks with broken T invariance.

The theoretical distributions of the real and imaginary parts of the off-diagonal element K_{ab} of the Wigner's reaction \hat{K} matrix are marked by red broken line. The error marks indicate the errors arising from the $\gamma = 5.39 \pm 0.23$ uncertainty. The experimental and theoretical distributions are in very good agreement. In this case the GF for the experimental distributions $P(u_1)$ and $P(u_2)$ to the theory [9] was 97.9% and 98.3%, respectively. Furthermore, in agreement with theory [9] the experimental distributions $P(u_i)$ of the real and imaginary parts of the off-diagonal element K_{ab} are very close to each other. Although, it is easily seen from Eq. (6) that the theory predicts both distributions to be identical, the exper-

imental confirmation of this property gives us an important validation of the experimental procedures. Figure 3(a) shows that for weakly overlapping resonances the distributions $P(u_i)$ are significantly different from the Gaussian approximation (blue solid line).

The observations for larger parameter $\gamma = 25.77 \pm 1.43$ are shown in Fig. 3(b). The experimental distributions $P(u_1)$ and $P(u_2)$ of the real and imaginary parts of the off-diagonal element K_{ab} of the Wigner's reaction \hat{K} matrix are denoted by black full circles and black triangles, respectively. The theoretical distribution is marked in Fig. 3(b) by a red broken line. The error bars estimate the error caused by the $\gamma = 25.77 \pm 1.43$ uncertainty. It is clearly seen that the experimental distributions $P(u_1)$ and $P(u_2)$ are in very good agreement with GUE predictions, with a high GF equal to 98.1% and 98.1%, respectively. Because the large parameter $\alpha = \gamma/4 = 6.44 \pm 0.36$ the Gaussian approximation (small blue circles) is much closer to the experimental and theoretical distributions $P(u_i)$ than in the case of much smaller parameter $\alpha = 1.35 \pm 0.06$, where a big discrepancy between the experiment and the Gaussian approximation was observed.

In summary, we have measured the distributions of the real and imaginary parts of the off-diagonal element of the scattering matrix S_{ab} for chaotic networks with broken time reversal symmetry and for different losses. The experimental results are in very good agreement with the theoretical predictions from supersymmetry random matrix theory [8]. We also experimentally determined the distributions of the real and imaginary parts of the off-diagonal element K_{ab} of the Wigner's reaction \hat{K} matrix for chaotic networks with broken time reversal symmetry. We show that K_{ab} is not Gaussian distributed when the levels do not completely overlap, in perfect agreement with recent theoretical prediction of Ref. [9].

ACKNOWLEDGMENTS

This work was supported in part by the National Science Centre, Poland, Grant No. UMO-2016/23/B/ST2/03979. L.S. thanks CNRS for support, Contract No. 874365. We would like to thank Yan Fyodorov, Szymon Bauch, and Pavel Kurasov for useful discussions.

-
- [1] E. P. Wigner, *Ann. Math.* **53**, 36 (1951).
 - [2] F. Haake, *Quantum Signatures of Chaos* (Springer-Verlag, Heidelberg, 2001).
 - [3] H. A. Weidenmüller and G. E. Mitchell, *Rev. Mod. Phys.* **81**, 539 (2009).
 - [4] M. V. Berry, *Proc. Roy. Soc. Lond. A* **400**, 229 (1985).
 - [5] O. Hul, S. Bauch, P. Pakoński, N. Savytskyy, K. Życzkowski, and L. Sirko, *Phys. Rev. E* **69**, 056205 (2004).
 - [6] M. Ławniczak, S. Bauch, O. Hul, and L. Sirko, *Phys. Rev. E* **81**, 046204 (2010).
 - [7] M. Ławniczak and L. Sirko, *Sci. Rep.* **9**, 5630 (2019).
 - [8] A. Nock, S. Kumar, H.-J. Sommers, and T. Guhr, *Ann. Phys. (NY)* **342**, 103 (2014).
 - [9] S. B. Fedeli and Y. V. Fyodorov, *J. Phys. A: Math. Theor.* **53**, 165701 (2020).
 - [10] L. Pauling, *J. Chem. Phys.* **4**, 673 (1936).
 - [11] T. Kottos and U. Smilansky, *Phys. Rev. Lett.* **79**, 4794 (1997).
 - [12] T. Kottos and U. Smilansky, *Phys. Rev. Lett.* **85**, 968 (2000).
 - [13] M. Ławniczak, O. Hul, S. Bauch, P. Sěba, and L. Sirko, *Phys. Rev. E* **77**, 056210 (2008).
 - [14] Z. Pluhař and H. A. Weidenmüller, *Phys. Rev. Lett.* **112**, 144102 (2014).
 - [15] O. F. Namarvar, G. Dridi, and C. Joachim, *Sci. Rep.* **6**, 30198 (2016).
 - [16] H. Z. Jooya, K. Reihani, and S.-I. Chu, *Sci. Rep.* **6**, 37544 (2016).
 - [17] M. Krenn, X. Gu, and A. Zeilinger, *Phys. Rev. Lett.* **119**, 240403 (2017).
 - [18] P. Arrighi and S. Martiel, *Phys. Rev. D* **96**, 024026 (2017).
 - [19] O. Hul, M. Ławniczak, S. Bauch, A. Sawicki, M. Kuś, and L. Sirko, *Phys. Rev. Lett.* **109**, 040402 (2012).
 - [20] M. Ławniczak, S. Bauch, and L. Sirko, in *Handbook of Applications of Chaos Theory*, edited C. Skiadas and C. Skiadas (CRC Press, Boca Raton, FL, 2016), p. 559.
 - [21] B. Dietz, V. Yunko, M. Białous, S. Bauch, M. Ławniczak, and L. Sirko, *Phys. Rev. E* **95**, 052202 (2017).
 - [22] M. Ławniczak, J. Lipovský, and L. Sirko, *Phys. Rev. Lett.* **122**, 140503 (2019).
 - [23] A. Rehemanjiang, M. Allgaier, C. H. Joyner, S. Müller, M. Sieber, U. Kuhl, and H.-J. Stöckmann, *Phys. Rev. Lett.* **117**, 064101 (2016).
 - [24] A. Rehemanjiang, M. Richter, U. Kuhl, and H.-J. Stöckmann, *Phys. Rev. E* **97**, 022204 (2018).
 - [25] J. Lu, J. Che, X. Zhang, and B. Dietz, *Phys. Rev. E* **102**, 022309 (2020).
 - [26] V. Yunko, M. Białous, and L. Sirko, *Phys. Rev. E* **102**, 012210 (2020).
 - [27] M. Białous, V. Yunko, S. Bauch, M. Ławniczak, B. Dietz, and L. Sirko, *Phys. Rev. Lett.* **117**, 144101 (2016).
 - [28] S. Kumar, A. Nock, H.-J. Sommers, T. Guhr, B. Dietz, M. Miski-Oglu, A. Richter, and F. Schäfer, *Phys. Rev. Lett.* **111**, 030403 (2013).
 - [29] S. Kumar, B. Dietz, T. Guhr, and A. Richter, *Phys. Rev. Lett.* **119**, 244102 (2017).
 - [30] B. Dietz, T. Klaus, M. Miski-Oglu, A. Richter, and M. Wunderle, *Phys. Rev. Lett.* **123**, 174101 (2019).
 - [31] Y. V. Fyodorov and D. V. Savin, *JETP Lett.* **80**, 725 (2004).
 - [32] D. V. Savin, H.-J. Sommers, and Y. V. Fyodorov, *JETP Lett.* **82**, 544 (2005).
 - [33] O. Hul, O. Tymoshchuk, S. Bauch, P. M. Koch, and L. Sirko, *J. Phys. A* **38**, 10489 (2005).
 - [34] S. Hemmady, X. Zheng, E. Ott, T. M. Antonsen, and S. M. Anlage, *Phys. Rev. Lett.* **94**, 014102 (2005).
 - [35] S. Hemmady, X. Zheng, T. M. Antonsen, Jr., E. Ott, and S. M. Anlage, *Acta Phys. Pol. A* **109**, 65 (2006).
 - [36] Y. V. Fyodorov and A. Nock, *J. Stat. Phys.* **159**, 731 (2015).
 - [37] I. Rozhkov, Y. V. Fyodorov, and R. L. Weaver, *Phys. Rev. E* **68**, 016204 (2003).

- [38] S. Hemmady, X. Zheng, J. Hart, T. M. Antonsen, Jr., E. Ott, and S. M. Anlage, *Phys. Rev. E* **74**, 036213 (2006).
- [39] M. Ławniczak, S. Bauch, O. Hul, and L. Sirko, *Phys. Scr. T* **143**, 014014 (2011).
- [40] Y. V. Fyodorov, D. V. Savin, and H. J. Sommers, *J. Phys. A* **38**, 10731 (2005).
- [41] M. L. Mehta, *Random Matrices* (Academic Press, London, 1990).
- [42] N. Savytskyy, A. Kohler, S. Bauch, R. Blümel, and L. Sirko, *Phys. Rev. E* **64**, 036211 (2001).
- [43] D. S. Jones, *Theory of Electromagnetism* (Pergamon Press, Oxford, 1964), p. 254.
- [44] P. Exner and P. Šeba, *Rep. Math. Phys.* **28**, 7 (1989).
- [45] P. Exner and M. Tater, *Phys. Lett. A* **382**, 283 (2018).
- [46] V. Kstrykin and R. Schrader, *J. Phys. A* **32**, 595 (1999).
- [47] P. Kurasov and M. Nowaczyk, *Opuscula Math.* **30**, 295 (2010).
- [48] G. Berkolaiko and P. Kuchment, *Introduction to Quantum Graphs, Mathematical Surveys and Monographs* (American Mathematical Society, Providence, 2013), Vol. 186, p. 270.
- [49] B. Dietz, T. Friedrich, H. L. Harney, M. Miski-Oglu, A. Richter, F. Schäfer, and H. A. Weidenmüller, *Phys. Rev. E* **81**, 036205 (2010).
- [50] Y. Kharkov and V. Sokolov, *Phys. Lett. B* **718**, 1562 (2013).
- [51] X. Zheng, S. Hemmady, T. M. Antonsen, Jr., S. M. Anlage, and E. Ott, *Phys. Rev. E* **73**, 046208 (2006).
- [52] R. Schäfer, T. Gorin, T. H. Seligman, and H. J. Stöckmann, *J. Phys. A* **36**, 3289 (2003).
- [53] T. Guhr, A. Müller-Groeling, and H. A. Weidenmüller, *Phys. Rep.* **299**, 189 (1998).